

Initial experience with X-ray CT based attenuation correction in myocardial perfusion SPECT imaging using a combined SPECT/CT system

Daisuke UTSUNOMIYA,^{***} Seiji TOMIGUCHI,^{**} Shinya SHIRAISHI,^{**} Koichiro YAMADA,^{*} Tsuyoshi HONDA,^{***}
Koichi KAWANAKA,^{**} Akihiro KOJIMA,^{****} Kazuo AWAI^{**} and Yasuyuki YAMASHITA^{**}

**Diagnostic Imaging Center, Saiseikai Kumamoto Hospital*

*Departments of **Diagnostic Radiology and ***Cardiovascular Medicine, Graduate School of Medical Sciences,
Kumamoto University*

*****Institute of Resource Development and Analysis, Kumamoto University*

Objective: Attenuation artifacts adversely affect the diagnostic accuracy of myocardial perfusion imaging. We assessed the clinical usefulness of X-ray CT based attenuation correction (AC) in patients undergoing myocardial perfusion imaging by comparing their myocardial AC- and non-corrected (NC) SPECT images with the coronary angiography (CAG). **Methods:** We retrospectively reviewed the myocardial SPECT images of 30 patients (18 men, 12 women; mean age 68 years). Thirteen of 30 patients with coronary artery disease (CAD) and 17 without CAD were confirmed by CAG. They underwent sequential CT and myocardial SPECT imaging with thallium-201 (111 MBq) under an exercise or pharmacological stress protocol using our combined SPECT/CT system. Two readers reviewed the myocardial SPECT images for the presence of CAD on a 4-point scale where 1 = normal, 2 = probably normal, 3 = probably abnormal, and 4 = abnormal. Two reading sessions were held. First, non-corrected (NC)-SPECT and second, AC-SPECT images using X-ray CT images were interpreted. Interobserver variability was assessed with kappa statistics. Diagnostic performance (accuracy) of coronary arterial stenosis was compared between AC- and NC-images. **Results:** Interobserver agreement for visual assessment was substantial or almost perfect. For AC-images, the observer consensus for analysis was 0.84 for the LAD-, 0.87 for the LCX-, and 0.71 for the RCA-territory. For NC-images, it was 0.91, 0.71, and 0.78. AC resulted in statistically significant improvements in overall diagnostic accuracy (sensitivity/specificity/accuracy = 76%/93%/89%, 67%/86%/81%, respectively, for AC- and NC-images). **Conclusions:** Because of an increase in the specificity, diagnostic accuracy was significantly increased on AC-images. These preliminary data suggest that X-ray CT based AC in myocardial SPECT imaging has the potential to develop into a reliable clinical technique.

Key words: coronary artery disease, myocardial perfusion SPECT, Tl-201, attenuation correction, CT

INTRODUCTION

STRESS-REST THALLIUM-201 (Tl-201) single-photon emission computed tomography (SPECT) is a well-established imaging method for evaluating the presence and

extent of coronary artery disease (CAD).^{1,2} However, the diagnostic accuracy of myocardial SPECT is adversely affected by specific physical effects including attenuation, scatter, and blur.^{3,4} Of these, attenuation artifacts are arguably the most serious in the assessment of myocardial perfusion.^{3,4} For non-uniform attenuators like those in the thorax, a patient-specific attenuation coefficient map is necessary.^{4,5} Transmission computed tomography (TCT) with an external gamma-ray source has been proposed^{3,6-8}; however, this method is not widely used in the clinical setting because it yields low-quality TCT images

Received January 26, 2005, revision accepted June 20, 2005.

For reprint contact: Daisuke Utsunomiya, M.D., Diagnostic Imaging Center, Saiseikai Kumamoto Hospital, 5-3-1 Chikami, Kumamoto 861-4193, JAPAN.

E-mail: d-utsunomiya@skh.saiseikai.or.jp

resulting from low photon flux, involves additional expense for software and hardware, and requires longer scan times.⁹ While attenuation coefficient maps generated from X-ray CT images⁹⁻¹¹ represent a simple, potentially useful clinical alternative, only a few studies have addressed the clinical usefulness of patient-specific attenuation correction (AC) using X-ray CT images.^{9,10}

In the present study we evaluated the clinical usefulness of X-ray CT based AC SPECT imaging using a SPECT/CT system. We compared myocardial perfusion SPECT images with and without AC based on the results of coronary angiographs performed for the diagnosis of coronary arterial stenosis.

METHODS

Patients

Using cases entered into our radiologic database between August 2003 and December 2003, we retrospectively reviewed stress-rest myocardial SPECT images obtained in 30 patients (18 men, 12 women; age 48–79 years; mean age 68 years) who had been examined with our combined SPECT/CT system. All patients referred for stress-rest myocardial SPECT imaging presented with atypical chest pain ($n = 18$) or were suspected of having myocardial ischemia based on the results of a treadmill exercise test ($n = 7$) or echocardiography ($n = 5$). They were recruited based on the following criteria: (a) no known CAD, (b) no coexisting valvular heart disease or cardiomyopathy, and (c) availability of CAG within two weeks after the stress-rest Tl-201 myocardial SPECT and X-ray CT images obtained with a SPECT/CT system. Of the 30 patients, 25 were exercise stress tested; the other 5 underwent pharmacologic stress testing. For emission, 111 MBq (3 mCi) of thallium-201 (Tl-201) was used in all patients. Imaging began within 15 min after the intravenous injection of Tl-201.

Our institutional review board approved both the multiple imaging studies and the retrospective analyses of these data; the protocol and the types of examinations were explained to all patients and their informed consent was obtained.

Data Acquisition and Processing

Figure 1 is a photograph of our combined SPECT/CT system with its adjacent gantry-free SPECT and multidetector CT scanners. As the examination table extends from the CT scanner into the gantry-free SPECT system, sequential imaging with both scanners is possible without having to reposition the patient. The gantry-free SPECT system was a Skylight (ADAC Laboratories, Milpitas, CA). Dual-head detectors were equipped with low-energy, general-purpose parallel-hole collimators; the heads were at 90 degrees to each other. A 30% window was centered at about 77 keV for the emission data. Projections were digitized onto a 64×64 matrix. A total

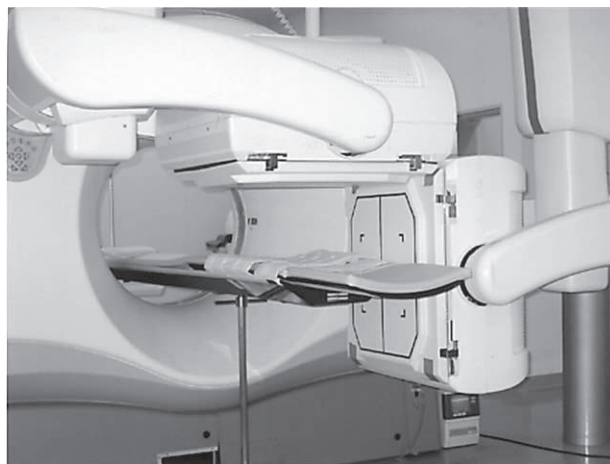


Fig. 1 Photograph of our combined SPECT/CT system with its adjacent SPECT and CT scanners without need for repositioning of the patient. The patient table from CT scanner extends into the gantry-free SPECT system.

of 32 projections were sampled over 90 degrees for each detector. Each view was acquired for 60 sec. The 8-row multidetector CT scanner was a LightSpeed Ultra (General Electric Medical System, Milwaukee, WI); the tube voltage was 120 kV, the tube electric current was 20 mA. The slice thickness was 5 mm, the rotation speed 4 sec/rotation under free breathing. The CT dose index (vol) was 6.8 mGy.

AC was performed with HYOGO CM software (Hyogo College of Medicine, Nishinomiya, Hyogo)⁹ on a Pegasus workstation (ADAC Laboratories). The process of AC was as follows: 1, image registration of the X-ray CT and SPECT images; 2, a creation of an X-ray CT-derived attenuation map; 3, the SPECT image reconstruction with AC by means of a maximum likelihood expectation maximization (ML-EM) algorithm. CT slice data were retrieved from an Advantage Windows 4.0P workstation (General Electric Medical System) via DICOM. CT slices were then converted into a SPECT-like data volume ($5.9 \text{ mm} \times 5.9 \text{ mm} \times 5.9 \text{ mm}$) for fusion of the SPECT and CT images. Registration of SPECT and CT images was performed manually by use of the margin of the heart as an internal marker by a radiologist (D.U.), and then the validity of image registration was evaluated on the computer display by two diagnostic radiologists (D.U. and S.T.) based on consensus. One (D.U.) had nine years experience and the other (S.T.) had 20 years experience in both nuclear medicine and CT imaging. After the CT images were registered with the SPECT images, the CT number was converted into the linear attenuation coefficient (μ) of Tl-201 (73 keV) on a pixel-by-pixel basis. The following equation was used for the relationship between CT number and μ (/cm): $\mu = 0.181 \times (\text{CT} + 1000)/1000$.

Using the attenuation coefficient map generated from the CT images, the AC SPECT images were created by the ML-EM method. Transaxial images were reformatted to

Table 1 Overall diagnostic accuracy for AC- and NC-images

| | Sensitivity | Specificity | Accuracy |
|----|-------------|-------------|-------------|
| AC | 16/21 (76%) | 64/69 (93%) | 80/90 (89%) |
| NC | 14/21 (67%) | 59/69 (86%) | 73/90 (81%) |

Note. AC = attenuation correction, NC = non correction

Table 2 Diagnostic accuracy for AC- and NC-images in each of three vascular territories

(LAD)

| | Sensitivity | Specificity | Accuracy |
|----|-------------|-------------|-------------|
| AC | 8/10 (80%) | 18/20 (90%) | 26/30 (87%) |
| NC | 7/10 (70%) | 19/20 (95%) | 26/30 (87%) |

(LCx)

| | Sensitivity | Specificity | Accuracy |
|----|-------------|-------------|-------------|
| AC | 4/6 (67%) | 23/24 (96%) | 27/30 (90%) |
| NC | 3/6 (50%) | 23/24 (96%) | 26/30 (87%) |

(RCA)

| | Sensitivity | Specificity | Accuracy |
|----|-------------|-------------|-------------|
| AC | 4/5 (80%) | 23/25 (92%) | 27/30 (90%) |
| NC | 4/5 (80%) | 17/25 (68%) | 21/30 (73%) |

Note. AC = attenuation correction, NC = non correction

produce short-axis, vertical long-axis, and horizontal long-axis displays. The reoriented reconstructed data sets and the Bull's eye display were then used for visual evaluation. For comparison, NC-SPECT images were also created by the ML-EM method.

Coronary Angiography

Cardiac catheterization was performed according to standard techniques, with access through the femoral or brachial artery. All segments of the coronary circulation were visualized in at least two projections. The resulting coronary angiograms were evaluated by an angiographer of seven years experience (T.H.). A notation of abnormal was made when at least one of the three major vascular territories (left anterior descending [LAD], left circumflex [LCX], right coronary artery [RCA]) exhibited luminal narrowing of 50% or greater.

Image Interpretation

Images were viewed on a computer monitor by two readers (T.N. and S.S.) blinded to the patients' age, and clinical status. Reader 1 (T.N.) had eight years experience and reader 2 (S.S.) had 10 years experience in nuclear cardiology. They were presented both in shades of gray and with a rainbow color scale. Grouped stress and rest studies were presented. The readers interpreted the images for the overall presence of CAD and its presence in each of the 3 main vascular territories (LAD, LCX, or

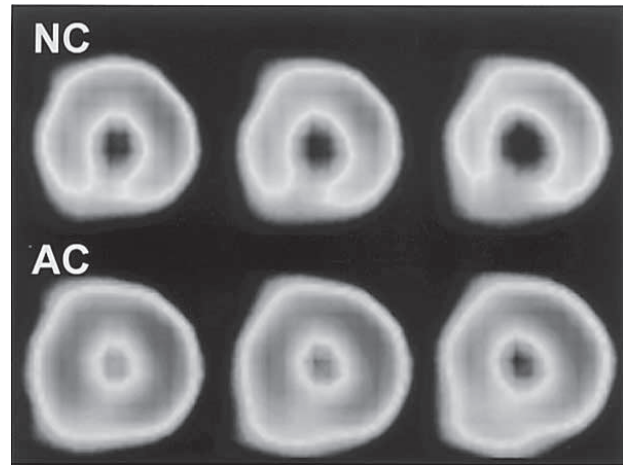


Fig. 2 Short-axial images of a 63-year-old female with normal coronary artery. In NC-images (*upper*), RCA territory shows decreased tracer uptake artifact. In AC-images (*lower*), RCA territory shows normal perfusion.

RCA) on a 4-point scale where 1 = normal, 2 = probably normal, 3 = probably abnormal, and 4 = abnormal. Two different reading sessions were held. In the first, NC-SPECT images, and in the second, two weeks after the first, AC-SPECT images were interpreted. Images were presented in random order to each of the readers at each session. Visual evaluations were performed independently so as to determine interobserver agreement between the two readers. In the absence of consensus, the more severe interpretation was accepted as the final determination. Interobserver variability was assessed with kappa statistics. Kappa values were reported as follows: 0 = agreement is a random effect; less than 0.20 = poor agreement; 0.21–0.40 = fair agreement; 0.41–0.60 = moderate agreement; 0.61–0.80 = substantial agreement; and 0.81–1.00 = almost perfect agreement.¹² The results of myocardial SPECT imaging were compared with those of CAG. We compared diagnostic accuracy between AC- and NC-SPECT images for the overall detection of CAD and for the localized detection of CAD in the LAD, LCX, and RCA territories. We used a scan score of 3 or 4 to indicate abnormal and a score of 1 or 2 to indicate normal in this analysis. McNemar's test was used to analyze the statistical significance of differences in assessing the diagnostic accuracy of each SPECT image. P values of less than 0.05 were considered statistically significant.

RESULTS

Of the 30 patients, 13 had CAD (8 single-vessel, 2 double-vessel, 3 three-vessel CAD). A total of 21 significant stenosis (10 in LAD, 6 in LCX and 5 in RCA, respectively) were present in these patients. The other 17 patients were normal by CAG. Diagnostic accuracy in the detection of coronary arterial stenosis was evaluated for

each territory and each patient. Interobserver agreement for visual assessment was substantial or almost perfect. For AC-images, the observer consensus for analysis was 0.84 for the LAD-, 0.87 for the LCX-, and 0.71 for the RCA territory. For NC-images, it was 0.91, 0.71, and 0.78. The overall diagnostic accuracy results are presented in Table 1. On AC-images, specificity and accuracy were higher than on NC-images and the difference in diagnostic accuracy was statistically significant (McNemar test, $p = 0.03$).

The diagnostic accuracy results in each of three vascular territories are presented in Table 2. In the RCA territory of the normal subject shown in Figure 2, AC yielded improved radioactivity in the inferior wall. Diagnostic accuracy was significantly higher on AC- than NC-images because of increased specificity in the RCA territory (McNemar test, $p = 0.01$). In the LAD and LCX territory, there was no significant difference between AC- and NC-images.

In 17 normal subjects, the percentages with the presence of artifacts of decreased tracer activities were 35% (6/17) and 12% (2/17), respectively, for NC- and AC-images. For NC-images, artifactual decreased perfusion was observed in the RCA- (5/6) and LAD territories (1/6). For AC-images, artifactual decreased perfusion was observed in the RCA- (1/2) and LAD territories (1/2).

DISCUSSION

Non-uniform AC is important in efforts to improve image quality and quantification measurements in myocardial perfusion SPECT imaging.^{3,9,13,14} In X-ray CT based AC, anatomically accurate image registration between SPECT and CT is essential.^{9,10} Our imaging system that combines a gantry-free gamma camera with a 8-row multidetector CT scanner allows for accurate image fusion between SPECT and CT. Compared to simultaneous transmission methods that employ external sources or hybrid scanners, the primary advantage of our SPECT/CT system is its ability to obtain high-quality anatomical images simultaneously. Multidetector CT is a promising method for the non-invasive visualization of coronary arteries.¹⁵ Image fusion of myocardial perfusion SPECT and coronary CT angiographic images will be important in future nuclear cardiology because it features both non-uniform AC and image fusion functions.

In our study, the increased accuracy of disease localization on AC-images resulted from an increase in the specificity in the RCA territory. Comparison of AC- and NC-images disclosed no changes in the specificity in the LAD or LCX territories. Ohyama et al.¹³ evaluated the clinical usefulness of AC for Tl-201 myocardial SPECT imaging using a three-detector SPECT system equipped with a Tc-99m line source and fan-beam collimators. Our results were similar to theirs, although our study population was relatively small. We suggest that X-ray CT

based AC is also useful in clinical practice. Vidal et al.¹⁶ reported that the increase in specificity obtained with AC in the RCA territory was accompanied by a significant decrease in the sensitivity of defect detection in the LAD territory. A decrease in sensitivity in the LAD territory on AC-images was not observed in this study. However, there was decreased tracer uptake in the LAD territory on the AC- but not the NC image in one normal subject on CAG. Reconstructed counts are artificially enhanced in the regions of high tissue density when scattered events are not removed from the projections prior to AC.^{13,17} This may be one of the main reasons why a decrease in activity appears in the LAD territory with AC. We postulate that over-correction of the inferior wall resulted in a relative decrease in tracer distribution in the LAD territory and we recommend the combined interpretation of AC- and NC-images. Furthermore, the addition of scatter correction may reduce the drawback of over-correction of the inferior wall.¹⁸

There are several limitations in our study. First, the conversion from CT values to the attenuation coefficient of gamma rays is complex because the energy spectrum of gamma rays is finite while X-rays are continuous. Second, our SPECT images were not scatter-corrected which would have improved image quality and the accuracy of quantification.^{19,20} Hendel et al.²¹ reported that while the specificity was significantly improved with attenuation/scatter correction and resolution compensation, the detection of coronary artery stenosis was similar on corrected and uncorrected perfusion data. Additional scatter and resolution compensation are desirable to avoid over-correction of the inferior wall that results in a relative decrease in tracer distribution in the LAD territory. Third, quantitative analysis was not performed in this study, because visual assessment of myocardial perfusion images is common in clinical practice. Fourth, we generated SPECT images with 180-degree data collection, chosen because anterior 180-degree acquisition is the standard in the clinical setting.²² Comparison between 180- and 360-degree acquisitions should be conducted. Fifth, the combined SPECT/CT system is not commonly used due to its increased cost and comparative lack of availability. In recent years, there has been considerable progress in the development of fusion software to co-register different imaging modalities.²³ The development of improved software algorithms is necessary to facilitate automatic and robust image fusion.

In conclusion, the diagnostic accuracy of the localization of CAD was higher on X-ray CT based AC-images than NC-images as evidenced by an increase in the specificity in the RCA territory. However, X-ray CT based AC- and NC-images did not differ significantly with respect to their diagnostic performance in the LAD or LCX territories. These preliminary data suggest that X-ray CT based AC in myocardial SPECT imaging has the potential to develop into a reliable clinical technique.

Additional studies are underway in our laboratory to test the usefulness of fusion imaging between myocardial AC-SPECT and coronary angiographic multidetector CT images.

REFERENCES

1. DePasquale EE, Nody AC, DePuey EG, Garcia EV, Pilcher G, Bredlau C, et al. Quantitative rotational thallium-201 tomography for identifying and localizing coronary artery disease. *Circulation* 1988; 77: 316–327.
2. Mahmarian JJ, Boyce TM, Goldberg RK, Cocanougher MK, Roberts R, Verani MS. Quantitative exercise thallium-201 single photon emission computed tomography for the enhanced diagnosis of ischemic heart disease. *J Am Coll Cardiol* 1990; 15: 318–329.
3. Tsui BM, Gullberg GT, Edgerton ER, Ballard JG, Perry JR, McCartney WH, et al. Correction of nonuniform attenuation in cardiac SPECT imaging. *J Nucl Med* 1989; 30: 497–507.
4. Kojima A, Tomiguchi S, Kawanaka K, Utsunomiya D, Shiraishi S, Nakaura T, et al. Attenuation correction using asymmetric fanbeam transmission CT on two-head SPECT system. *Ann Nucl Med* 2004; 18: 315–322.
5. Tung CH, Gullberg GT. A simulation of emission and transmission noise propagation in cardiac SPECT imaging with nonuniform attenuation correction. *Med Phys* 1994; 21: 1565–1576.
6. Jaszczak RJ, Gilland DR, Hanson MW, Jang S, Greer KL, Coleman RE. Fast transmission CT for determining attenuation maps using a collimated line source, rotatable air-copper-lead attenuators and fan-beam collimation. *J Nucl Med* 1993; 34: 1577–1586.
7. Ficaro EP, Fessler JA, Rogers WL, Schwaiger M. Comparison of americium-241 and technetium-99m as transmission sources for attenuation correction of thallium-201 SPECT imaging of the heart. *J Nucl Med* 1994; 35: 652–663.
8. Ficaro EP, Fessler JA, Ackermann RJ, Rogers WL, Corbett JR, Schwaiger M. Simultaneous transmission-emission thallium-201 cardiac SPECT: effect of attenuation correction on myocardial tracer distribution. *J Nucl Med* 1995; 36: 921–931.
9. Kashiwagi T, Yutani K, Fukuchi M, Naruse H, Iwasaki T, Yokozuka K, et al. Correction of nonuniform attenuation and image fusion in SPECT imaging by means of separate X-ray CT. *Ann Nucl Med* 2002; 16: 255–261.
10. Takahashi Y, Murase K, Higashino H, Mochizuki T, Motomura N. Attenuation correction of myocardial SPECT images with X-ray CT: effects of registration errors between X-ray CT and SPECT. *Ann Nucl Med* 2002; 16: 431–435.
11. Fleming JS. A technique for using CT images in attenuation correction and quantification in SPECT. *Nucl Med Commun* 1989; 10: 83–97.
12. Svanholm H, Starklint H, Gundersen HJ, Fabricius J, Barlebo H, Olsen S. Reproducibility of histomorphologic diagnoses with special reference to the kappa statistic. *Apmis* 1989; 97: 689–698.
13. Ohyama Y, Tomiguchi S, Kira T, Kira M, Tsuji A, Kojima A, et al. Diagnostic accuracy of simultaneous acquisition of transmission and emission data with technetium-99m transmission source on thallium-201 myocardial SPECT. *Ann Nucl Med* 2001; 15: 21–26.
14. Duvernoy CS, Ficaro EP, Karabajakian MZ, Rose PA, Corbett JR. Improved detection of left main coronary artery disease with attenuation-corrected SPECT. *J Nucl Cardiol* 2000; 7: 639–648.
15. Schoenhagen P, Halliburton SS, Stillman AE, Kuzmiak SA, Nissen SE, Tuzcu EM, et al. Noninvasive imaging of coronary arteries: current and future role of multi-detector row CT. *Radiology* 2004; 232: 7–17.
16. Vidal R, Buvat I, Darcourt J, Migneco O, Desvignes P, Baudouy M, et al. Impact of attenuation correction by simultaneous emission/transmission tomography on visual assessment of ²⁰¹Tl myocardial perfusion images. *J Nucl Med* 1999; 40: 1301–1309.
17. Meikle SR, Hutton BF, Bailey DL. A transmission-dependent method for scatter correction in SPECT. *J Nucl Med* 1994; 35: 360–367.
18. Harel F, Genin R, Daou D, Lebtahi R, Delahaye N, Helal BO, et al. Clinical impact of combination of scatter, attenuation correction, and depth-dependent resolution recovery for (201)Tl studies. *J Nucl Med* 2001; 42: 1451–1456.
19. Khalil ME, Brown EJ Jr, Heller EN. Does scatter correction of cardiac SPECT improve image quality in the presence of high extracardiac activity? *J Nucl Cardiol* 2004; 11: 424–432.
20. Kojima A, Kawanaka K, Nakaura T, Shiraishi S, Utsunomiya D, Katsuda N, et al. Attenuation correction using combination of a parallel hole collimator and an uncollimated non-uniform line array source. *Ann Nucl Med* 2004; 18: 385–390.
21. Hendel RC, Berman DS, Cullom SJ, Follansbee W, Heller GV, Kiat H, et al. Multicenter clinical trial to evaluate the efficacy of correction for photon attenuation and scatter in SPECT myocardial perfusion imaging. *Circulation* 1999; 99: 2742–2749.
22. DePuey EG, Garcia EV. Updated imaging guidelines for nuclear cardiology procedures. Part 1. *J Nucl Cardiol* 2001; 8: G1–G58.
23. Townsend DW, Cherry SR. Combining anatomy and function: the path to true image fusion. *Eur Radiol* 2001; 11: 1968–1974.